Inorganic Chemistry
Article
pubs.acs.org/IC

Aldehyde Deformylation and Catalytic C−H Activation Resulting from a Shared Cobalt(II) Precursor

Qiao Zhang, Angela Bell-Taylor, Fraser M. Bronston, John D. Gorden, and Christian R. Goldsmith*

Department of Chemistry and Biochemistry, Auburn University, Auburn, Alabama 36849, United States

Supporting Information

ABSTRACT: The tetradentate ligand *N*,*N*′-dibenzyl-*N*,*N*′-bis(2-pyridylmethyl)-1,2-cyclohexanediamine (bbpc) was used to prepare cobalt(II) diacetonitrilo and cobalt(III) peroxo complexes, the latter of which was structurally characterized. The cobalt(III) peroxo compound forms from reactions between the cobalt(II) complex, hydrogen peroxide, and a base, and it stoichiometrically reacts with aldehydes to yield mixtures of alkenes and ketones. The cobalt(II) precursor is capable of catalyzing the activation of weak C−H bonds by either iodosobenzene or *m*-chloroperbenzoic acid. This chemistry differs from most previously characterized cobalt-mediated C−H activation in that (1) it is catalytic, rather than stoichiometric, with respect to the cobalt and (2) it does not need a second Lewis acid metal ion in order to proceed.

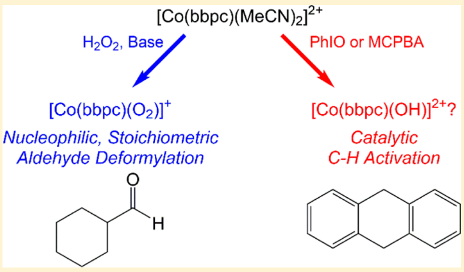

INTRODUCTION

The interactions between dioxygen (O_2) and metal ions continue to fascinate chemists even after decades of study. Metal−O_2 adducts have been characterized in a wide variety of biomolecules, including several classes of oxido-reductase enzymes, as well as their functional small-molecule mimics.[1−10] Such species are also highly relevant to those studying the metal-catalyzed oxidation of water (H_2O) to dihydrogen and O_2[11−16] and the oxidation of hydrocarbon substrates by O_2.[17−23] In the recently reported cobalt-catalyzed H_2O oxidation, binuclear cobalt(IV) oxo species are proposed as key intermediates for O_2 generation;[12,13] a binuclear cobalt(III) peroxo species could conceivably result upon formation of the first of the two O−O bonds (Scheme 1). A prior report implicated the agency of a mononuclear Co(IV)-oxo species in cobalt-catalyzed O_2 production from tris(2,2′-bipyridine)ruthenium(III) and H_2O.[15]

Scheme 1

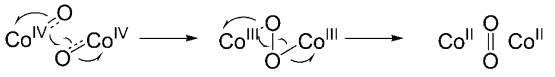

In recent years, many advances have been made with respect to the preparation of coordination complexes with ligands that can potentially be derived from O_2. Nam, Que, and co-workers have used a series of tetramethylated macrocycles (TMCs, Scheme 2) to stabilize a widening range of complexes relevant to O_2 activation that include metal oxo, peroxo, and hydroperoxo compounds.[24−35] The stabilities and reactivities of these with organic molecules have been found to depend on the identity of the ligand,[28−30] but clarification of the structure−function relationships remains an ongoing process. The metal peroxo complexes with TMCs and other ligands have been found to behave as nucleophiles,[29,31−36] but a recent report noted that protonating a cobalt(III) peroxo complex to a cobalt(III) hydroperoxo species enables the oxidation of weak C−H bonds.[35]

Scheme 2

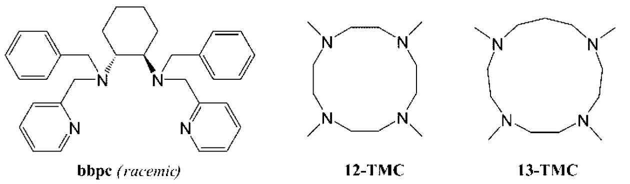

Metal oxo complexes have been found to participate in oxygen-atom-transfer and hydrogen-atom-abstraction reactions.[24,37−43] Ray's research group recently reported a cobalt(IV) oxo species with a tripodal tetradentate ligand,[44] but subsequent research from the Borovik group suggested that this may instead be better assigned as a Co^{III}-OH complex.[45] The debate about the identity of this species highlights that extreme caution must be taken when making such assignments for metal ions close to the "oxo wall".[16,46,47] The higher-valent oxidants generated from the cobalt(II) precursors by the aforementioned groups require Lewis acid additives to form and react stoichiometrically with weak C−H bonds, such as the benzylic ones in 9,10-dihydroanthracene.[44,45] A cobalt(II) complex reported by the Tilley group reacts with O_2 and other terminal oxidants to activate the much stronger C−H bonds in acetonitrile (MeCN).[48] A cobalt(IV) oxo species was proposed to be responsible for the C−H activation; the cobalt(III) superoxo complex initially formed from the reaction between

Received: September 6, 2016

DOI: 10.1021/acs.inorgchem.6b02127

cobalt(II) and O_2 is unlikely to be a strong enough oxidant to abstract a hydrogen atom from MeCN.[49]

Previous work from our group used the ligand *N,N*′-dibenzyl-*N,N*′-bis(2-pyridylmethyl)-1,2-cyclohexanediamine (bbpc; Scheme 2) to prepare an Fe^{III}-OOH complex from both O_2 and hydrogen peroxide (H_2O_2).[18,50] The steric bulk of the ligand modulates the regioselectivity of the iron-catalyzed oxidation of hydrocarbons by H_2O_2 and sufficiently stabilizes the Fe^{III}-OOH species for extensive characterization.[18,50,51] Kinetic analysis of the formation of this compound suggests that the O_2 chemistry may proceed through an iron(III) superoxo species.[18,51] In the current work, we use the bbpc ligand to prepare stable cobalt(II) and cobalt(III) peroxo complexes. We subsequently interrogated the reactivities of these species with various terminal oxidants and small-molecule substrates and found that the bbpc ligand, much like 12-TMC,[35] could support the formation of both electrophilic and nucleophilic metal-based oxidants from a shared cobalt(II) precursor.

■ EXPERIMENTAL SECTION

Materials. Cobalt(II) perchlorate hexahydrate ($Co(ClO_4)_2{\cdot}6H_2O$), triethylamine (Et_3N), benzaldehyde, 4-chlorobenzaldehyde, 1,2-dichlorobenzene, xanthene, 9,10-dihydroanthracene (DHA), anthracene, 1,4-cyclohexadiene (CHD), acetophenone, cyclohexanone, cyclohexene, and *m*-chloroperbenzoic acid (MCPBA) were purchased from Sigma-Aldrich. Acetonitrile (MeCN), cyclohexanecarboxaldehyde (CCA), and triphenylphosphine (PPh_3) were purchased from Acros Organics. 2-Phenylpropionaldhyde (2-PPA), iodosobenzene (PhIO), 4-fluorobenzaldehyde, and *p*-tolualdehyde were obtained from TCI America. All deuterated solvents were purchased from Cambridge Isotopes. Methanol (MeOH) and ethanol were acquired from Pharmaco-Aaper and EMD Chemicals, respectively. Hydrogen peroxide (H_2O_2; 50 wt %) was bought from Fisher Chemical and calibrated by titration of $KMnO_4$ and H_2SO_4 in H_2O. *N,N*′-Dibenzyl-*N,N*′-bis(2-pyridylmethyl)-1,2-cyclohexanediamine (bbpc) was synthesized as described previously.[50] PhIO was kept in a 253 K freezer when not in use. H_2O_2 and MCPBA were kept in a 277 K refrigerator when not in use.

Instrumentation. ^{1}H NMR spectra were recorded on either a 400 MHz or a 250 MHz AV Bruker NMR spectrometer at 294 K. A Varian Cary 50 spectrophotometer was used to collect optical data, which were processed and analyzed using software from the WinUV Analysis Suite. IR data were obtained using a Shimadzu IR Prestige-21 FT-IR spectrophotometer. A Thermo Scientific Trace GC ultra gas chromatograph and Thermo Scientific TR-1 and TG-WAXMS columns were used for gas chromatography (GC). A Johnson Matthey magnetic susceptibility balance (model MK I#7967) was used to measure the magnetic moments of solid samples. Pascal's constants were used to estimate the diamagnetic correction to the susceptibility.[52] Electron paramagnetic resonance (EPR) spectra were collected on a Bruker EMX-6/1 X-band EPR spectrometer operated in the perpendicular mode. High-resolution mass spectrometry (MS) data were collected at the Mass Spectrometer Center at Auburn University on a Bruker microflex LT MALDI-TOF mass spectrometer via direct probe analysis operated in the positive-ion mode. Crystalline samples were dried, stored under N_2, and sent to Atlantic Microlabs (Norcross, GA) for elemental analysis.

Crystallographic Studies. Single crystals of $[Co(bbpc)(O_2)](ClO_4)$ (**2**) were mounted on CryoLoops with Krytox oil and optically aligned on a Bruker APEXII Quazar X-ray diffractometer using a digital camera. Initial intensity measurements were performed using an IμSX-ray source and a 30 W microfocused sealed tube (Mo Kα, λ = 0.71073 Å) with high-brilliance and high-performance focusing Quazar multilayer optics. Standard *APEXII* software was used for determination of the unit cells and data collection control. The intensities of the reflections of a sphere were collected by a combination of four sets of exposures (frames). Each set had a different φ angle for the crystal, and each exposure covered a range of 0.5° in ω. A total of 1464 frames were collected with an exposure time per frame of 20−60 s, depending on the crystal. The *SAINT* software was used for data integration including Lorentz and polarization corrections. Semiempirical absorption corrections were applied using the program *SADABS* or *TWINABS*. Selected crystallographic information is listed in Tables 1 and 2. Atomic coordinates and additional structural information are provided as Supporting Information.

Table 1. Selected Crystallographic Data for 2

empirical formula	$[Co(bbpc)(O_2)](ClO_4)$
formula	$C_{68}H_{72}Cl_2Co_2N_{10}O_{13}$
MW	1426.12
cryst syst	triclinic
space group	$P\bar{1}$ (No. 2)
a (Å)	13.7667(11)
b (Å)	15.0930(13)
c (Å)	17.3669(15)
α (deg)	97.363(2)
β (deg)	105.117(2)
γ (deg)	103.647(2)
V (Å^3)	3315.4(5)
Z	4
cryst color	red
T (K)	198
reflns collected	42371
unique reflns	10837
R1(F) [$I > 2\sigma(I)$][a]	0.0948
wR2(F^2) (all data)[a]	0.2774

[a] $R1 = \sum||F_o| - |F_c|| / \sum|F_o|$; $wR2 = [\sum w(F_o^2 - F_c^2)^2 / \sum wF_o^4]^{1/2}$.

Synthesis. ***Caution!*** *Perchlorate salts of metal complexes are potentially explosive and should be handled with care. Precautionary measures include working with small quantities and low concentrations of these reagents. Appropriate safety measures, such as protective shields, should be employed during their syntheses and subsequent handling.*

bbpc. IR data were collected for this compound. IR (KBr, cm^{-1}): 3002 (w), 2937 (w), 2805 (w), 1963 (w), 1734 (w), 1587 (m), 1567 (m), 1494 (m), 1473 (m), 1451 (m), 1362 (m), 1307 (m), 1264 (m), 1212 (m), 1147 (s), 1114 (s), 1092 (s), 1073 (s), 1045 (s), 1027 (s), 997 (s), 969 (s), 945 (s), 918 (m), 850 (s), 824 (s), 768 (s), 702 (s), 654 (m), 618 (m), 567 (s), 535 (s), 478 (s), 443 (m).

cis-Diacetonitrilo[N,N′-dibenzyl-N,N′-bis(2-pyridylmethyl)-1,2-cyclohexanediamine]cobalt(II) Perchlorate ($[Co^{II}(bbpc)(MeCN)_2](ClO_4)_2$, ***1****).* The bbpc ligand (0.476 g, 1.00 mmol) and $Co(ClO_4)_2{\cdot}6H_2O$ (0.366 g, 1.00 mmol) were dissolved in 10 mL of MeCN and stirred for 2 h. After this time, the solvent was removed through rotavaporation. The red residue was dissolved in 2.5 mL of fresh MeCN. The gradual diffusion of Et_2O into the solution deposited red crystals of the product (0.693 g, 85%) that were not suitable for single-crystal X-ray diffraction. Solid-state magnetic susceptibility (294 K): μ_{eff} = 3.9 μ_B. Optical spectroscopy [MeCN, 294 K; λ, nm (ε, M^{-1} cm^{-1})]: 258 (7850), 475 (50). ^{1}H NMR (CD_3CN, 294 K, 400 MHz): δ 95.0, 86.6, 84.0, 82.4, 78.6, 75.9, 74.3, 72.4, 67.8, 66.5, 63.3, 59.4, 58.8, 48.3, 40.0, 38.1, 35.2, 32.2, 31.5, 27.7, 25.1, 23.2, 22.5, 21.0, 19.3, 16.4, 15.1, 14.0, 13.4, 12.4, 11.3, 10.0, −1.1, −1.5, −3.4, −4.6, −11.1, −13.1, −13.7, −25.3. EPR (MeCN, 4 K): g = 4.3. IR (KBr, cm^{-1}): 3439 (m), 2938 (w), 2863 (w), 2026 (w), 1695 (s), 1610 (s), 1484 (m), 1449 (s), 1384 (m), 1352 (m), 1311 (w), 1297 (w), 1206 (m), 1145 (s), 1122 (s), 977 (m), 930 (w), 884 (w), 828 (w), 762 (s), 708 (m), 625 (s). Elem anal. Calcd for $C_{36}H_{42}CoCl_2N_6O_8{\cdot}2H_2O$: C, 50.71; H, 5.44; N, 9.86. Found: C, 50.96; H, 5.30; N, 9.86.

η^2-Peroxo[N,N′-dibenzyl-N,N′-bis(2-pyridylmethyl)-1,2-cyclohexanediamine]cobalt(III) Perchlorate ($[Co^{III}(bbpc)(O_2)](ClO_4)$, ***2****).* A solution of H_2O_2 (31 μL, 0.50 mmol) in 1.0 mL of MeCN was added to a solution of **1** (82 mg, 0.10 mmol) and Et_3N (35 μL, 0.25

Table 2. Selected Bond Lengths (Å) and Angles (deg) for 2[a]

bond length	cation A	cation B	bond angle	cation A	cation B
Co−N(1)	1.961(6)	1.954(6)	O(1)−Co−O(2)	46.1(2)	45.5(2)
Co−N(2)	2.012(6)	2.012(6)	O(1)−Co−N(1)	104.9(2)	104.2(2)
Co−N(3)	1.982(6)	1.984(6)	O(1)−Co−N(2)	93.5(2)	93.6(2)
Co−N(4)	1.910(6)	1.919(7)	O(1)−Co−N(3)	157.1(2)	157.6(2)
Co−N_{avg}	1.966	1.967	O(1)−Co−N(4)	95.5(3)	95.0(3)
Co−O(1)	1.863(5)	1.864(5)	O(2)−Co−N(1)	151.0(2)	149.8(2)
Co−O(2)	1.860(5)	1.849(5)	O(2)−Co−N(2)	95.6(2)	95.5(2)
Co−O_{avg}	1.862	1.857	O(2)−Co−N(3)	111.0(2)	112.1(2)
O(1)−O(2)	1.458(7)	1.437(7)	O(2)−Co−N(4)	90.7(2)	90.5(2)
			N(1)−Co−N(2)	84.3(3)	84.3(3)
			N(1)−Co−N(3)	98.0(3)	98.1(3)
			N(1)−Co−N(4)	93.2(3)	93.6(3)
			N(2)−Co−N(3)	87.8(2)	87.7(3)
			N(2)−Co−N(4)	171.0(3)	171.4(3)
			N(3)−Co−N(4)	84.0(3)	84.3(3)

[a] N(1) and N(4) correspond to pyridine nitrogen atoms; N(2) and N(3) correspond to amine nitrogen atoms. The donor atoms of cation B have been relabeled from their CIF assignments in order to facilitate comparison to their counterparts in cation A.

Scheme 3. Proposed Structures of Co(bbpc) Complexes

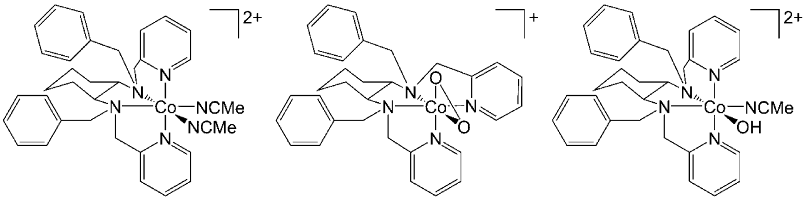

$[Co(bbpc)(MeCN)_2]^{2+}$ (**1**) $[Co(bbpc)O_2]^{+}$ (**2**) $[Co(bbpc)(MeCN)(OH)]^{2+}$ (**3**)

mmol) in 9.0 mL of MeCN at 273 K. After 5 min, the solvent and excess Et_3N were removed through rotavaporation to yield a dark-red solid. Crystalline product was obtained from the diffusion of Et_2O into a solution of the crude in MeCN at 253 K (49 mg, 74%). Optical spectroscopy [MeCN, 294 K; λ, nm (ε, M^{-1} cm^{-1})]: 320 (3100), 505 (350). ^1H NMR (CD_3CN, 294 K, 400 MHz): δ 8.08 (1H, t, J = 7.8 Hz), 7.78 (2H, d, J = 7.2 Hz), 7.67 (1H, d, J = 8.0 Hz), 7.45 (8H, m), 7.18 (1H, d, J = 5.2 Hz), 7.09 (4H, m), 6.49 (1H, d, J = 7.6 Hz), 5.19 (1H, d, J = 12 Hz), 4.63 (1H, d, J = 12 Hz), 4.58 (1H, d, J = 16 Hz), 4.02 (2H, dd, J_1 = 16 Hz, J_2 = 5.8 Hz), 3.79 (1H, d, J = 16 Hz), 3.68 (1H, d, J = 14 Hz), 3.44 (1H, t, J = 5.4 Hz), 3.32 (1H, d, J = 14 Hz), 2.57 (1H, t, J = 12 Hz), 2.09 (substantial overlap with the MeCN peak prevents accurate integration, t, J = 4.8 Hz), 1.67 (1H, d, J = 14 Hz), 1.31 (1H, d, J = 12 Hz), 1.1−0.79 (5H, m). IR (KBr, cm^{-1}): 3424 (m), 2938 (w), 2861 (w), 1605 (s), 1448 (m), 1384 (m), 1352 (m), 1295 (w), 1261 (w), 1146 (s), 1122 (s), 1119 (s), 941 (w), 929 (w), 803 (m), 762 (m), 706 (m), 625 (s). MS (ESI). Calcd for M^+: m/z 567.2170. Found: m/z 567.2093. Elem anal. Calcd for $C_{32}H_{36}ClCoN_4O_6\cdot1.5H_2O$: C, 55.38; H, 5.66; N, 8.07. Found: C, 55.10; H, 5.37; N, 8.04.

Reactivity. Unless stated otherwise, all reactivity studies were done at 298 K in MeCN under air. The yields of organic products were determined by GC; all reported values are the average of at least three independent measurements. The listed errors represent one standard deviation. The identities and yields of products were confirmed by comparing the GC retention times with those of authentic compounds and by comparing the peak integrations with that of a nonreactive 1,2-dichlorobenzene internal standard.

For the reactions between **2** and aldehydes, complex **2** was made in situ from 2.0 mM **1**, 10 mM H_2O_2, and 5.0 mM Et_3N in MeCN, as was done for an earlier study of cobalt(III) peroxo reactivity.[29] The disappearance of **2** was followed by monitoring the local absorbance maximum at 505 nm; pseudo-first-order rate constants, k_{obs}, were calculated from these data. At least three values of k_{obs} were measured per concentration of the aldehyde substrate. The listed k_2 values were obtained from plots of k_{obs} versus the concentration of the aldehyde substrates.

For the C−H activation reactions, the cobalt(II) compound **1**, unreactive internal standard, and hydrocarbon substrate were dissolved in 2.5 mL of MeCN, with initial concentrations of 1.0 and 50 mM, respectively. A total of 25 equiv of either PhIO or MCPBA were added as a solid, after which the reaction vessel was sealed. During the reaction, aliquots were removed via syringe, diluted with ether, filtered through silica gel, and analyzed via GC.

■ RESULTS

Synthesis and Spectroscopic Characterization. The cobalt(II) species **1** (Scheme 3) forms readily from mixtures of bbpc and $Co(ClO_4)_2\cdot6H_2O$. The complex can be isolated in high yields through precipitation from $MeCN/Et_2O$ mixtures. Attempts to crystallize this species have thus far been unsuccessful, even with alternative counteranions. The material is highly hygroscopic and needs to be dried under a vacuum in order to remove most of the adventitious H_2O. The magnetic susceptibility of solid-state samples is consistent with a μ_{eff} value of 3.9 μ_B and a high-spin d^7 metal center. As anticipated, the ^1H NMR spectrum of **1** is consistent with a paramagnetic species, with peaks ranging from −30 to +100 ppm (Figure S1). The number of peaks exceeds the number of hydrogen atoms on the bbpc ligand and suggests that multiple conformational or solvate isomers are present. Complex **1** is EPR-silent at 77 K but displays a feature at g = 4.3 at 4 K (Figure S2), similar to that observed for other high-spin cobalt(II) complexes.[53,54] Unlike its iron-containing analogue and some cobalt(II) complexes with other pyridylamine ligands, **1** does not react rapidly with O_2, even in the presence of substrates with weak allylic and benzylic C−H bonds.[18,55] The cobalt(II) complex can be stored for several weeks under air without any evidence of degradation, but a sample that was stored under air for approximately one year partly decomposed over this time, as evidenced by changes to its UV/vis spectrum. The MeCN ligands exchange readily, and markedly different UV/vis spectra are obtained when the compound is dissolved in other coordinating solvents, such as MeOH (Figure S3).

Complex **1** can be oxidized to **2** (Scheme 3) upon reaction with slight excesses of H_2O_2 and Et_3N. Upon oxidation, the dark-red solutions of **2** persist at room temperature with no noticeable discoloration for several hours. Although the compound can be precipitated in high yields, we limited the scale of the reaction to under 100 mg because of the potential explosive hazards associated with the peroxides and perchlorate salts. The isolated **2** is diamagnetic, as assessed by ^{1}H NMR (Figure S4) and the absence of an EPR signal. The UV/vis absorption shoulder at 505 nm clearly distinguishes **2** from the other cobalt species in this paper and gives the solid a dark-red color (Figure S3). Attempts to obtain resonance Raman data capable of providing further insight into the strength and electronic character of the O−O bond were unsuccessful. Both cobalt complexes and the free bbpc ligand have bands between 800 and 900 cm^{-1} in their IR spectra (Figures S5−S7), preventing us from definitively assigning any of these peaks to O−O stretches.

The ^{1}H NMR spectrum of **2** indicates that the ligand is bound asymmetrically to the metal center (Figure S4). The pyridine rings are inequivalent, as are the methylene groups connecting the benzyl and pyridine rings to the diamine. Because free motion of the benzyl groups would be anticipated to coalesce the benzylic peaks into singlets, the splitting patterns associated with these peaks suggest that their mobility is limited, even in solution.

Complex **1** appears to be oxidized to another higher-valent species upon reaction with PhIO. ^{1}H NMR analysis of the reaction mixture shows that much of PhIO has reacted to form PhI, demonstrating that the reaction does not halt at a simple Co^{II}-PhIO adduct (Figures S8 and S9). The ^{1}H NMR spectrum otherwise lacks well-resolved diamagnetic features. MS analysis of the reaction between **1** and PhIO revealed a m/z 296.6 feature consistent with $[Co(bbpc)(MeCN)(OH)]^{2+}$ (**3**; predicted m/z 296.6; Scheme 3), but this is a minor portion of the spectrum (Figures S12 and S13). When PhIO is premixed with ^{18}O-labeled H_2O, the peak at m/z 297.6 intensifies, consistent with the incorporation of ^{18}O into the complex. To our chagrin, attempts to isolate this species in a solid form failed. Removal of the solvent resulted in a brown oil, as did the introduction of nonpolar solvents into MeOH and MeCN solutions. Other features observed by MS are consistent with ligand oxidation, specifically the loss of either a benzyl or phenyl group and/or dehydrogenation of the C−N bonds to C═N groups (Figure S12). The data suggest that the metal-based oxidant does not accumulate to a high enough level to allow for its isolation.

Crystal Structure of the Cobalt(III) Peroxo Complex. The cobalt(II) complex **1** precipitates as a microcrystalline material, but we were unable to obtain sufficiently high-quality crystals for characterization by X-ray diffraction. The cobalt(III) peroxo complex **2**, conversely, was successfully characterized by this technique (Table 1).

Each unit cell in the structure contains two independent cations with the formula $[Co(bbpc)(O_2)]^+$. In each cation, the cobalt is coordinated in a highly distorted octahedral geometry, with the greatest distortions deriving from the small bite angles associated with the κ_2-peroxo ligand (Figure 1 and Table 2). Each bbpc ligand wraps around a single cobalt atom in a cis-β conformation, which places the two pyridine rings cis to each other. Three previously characterized coordination complexes with the bbpc ligand instead displayed either the cis-α conformation, in which the terminal binding groups of the tetradentate ligand are trans to each other, or the trans conformation, in which the donors from the tetradentate ligand are approximately coplanar.[50] In both $[Co(bbpc)(O_2)]^+$ cations, one of the benzyl rings from the bbpc ligand orients roughly parallel to a metal-bound pyridine ring, possibly indicating intramolecular aromatic interactions between the two (Figure 1). For both cations, the centroids of the phenyl and pyridine rings are 3.78 Å apart. The metal−ligand bond distances are consistent with low-spin cobalt(III) metal centers (Table 2).[29,56−60] The 1.46 and 1.44 Å O−O bond lengths from the two molecules in the unit cell are both consistent with single bonds between the oxygen atoms and are similar to values measured for other cobalt(III) peroxo complexes.[29,56−59] The ^{1}H NMR and MS data (Figure S11) collected for **2** suggest that the structure is maintained in solution.

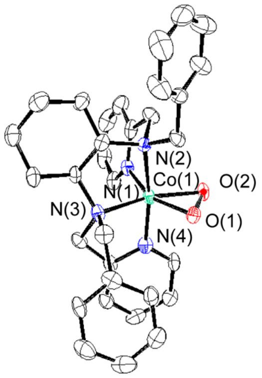

Figure 1. ORTEP representation of cation A, $[Co(bbpc)(O_2)]^+$, in the crystal structure of **2**. Hydrogen atoms, solvent molecules, perchlorate counteranions, and cation B have been omitted for clarity. All thermal ellipsoids are drawn at 50% probability. The cobalt atom has been relabeled from its original CIF designation.

Reactivity of the Cobalt(III) Peroxo Species. Complex **2** was tested for its ability to participate in a variety of different reactions. The cobalt(III) peroxo species is not a competent electrophile, and it is unable to abstract hydrogen atoms even from benzylic and allylic substrates, such as xanthene, DHA, and cyclohexene. The lack of reactivity was confirmed by both UV/vis and GC analyses of the reaction mixtures, the latter of which showed no substrate oxidation. Complex **2** was likewise unable to convert alkenes, such as cyclooctene and cyclohexene, into epoxides.

The Co^{III}-O_2 species, conversely, is a competent nucleophile. Much like previously characterized M^{III}-O_2 compounds, **2** reacts with aldehydes in MeCN at 298 K (Table 4).[28,29,31,36] In these studies, the cobalt(III) peroxo complex was generated in situ, largely to facilitate comparisons to earlier studies.[61] CCA is converted to a mixture of cyclohexene and cyclohexanone in yields of 26 (±6)% and 63 (±10)%, respectively. With a large excess of CCA, the chromophore associated with **2** undergoes first-order decay (Figure S14). The reaction is first-order with respect to CCA (Figure 2), and analysis of the relationship between k_{obs} and the concentration of the aldehyde yields a k_2 value of 2.4 (±0.2) × 10^{-2} M^{-1} s^{-1}. Complex **2** converts 2-PPA

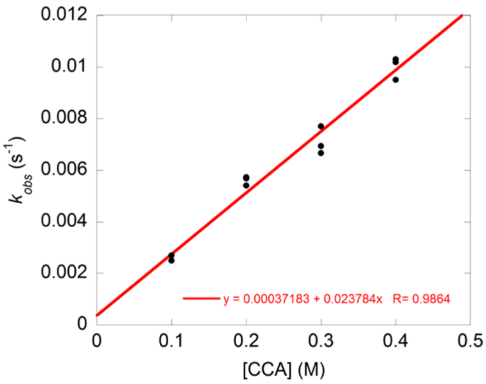

Figure 2. Plot of observed rate constants (k_{obs}) for the pseudo-first order decay of **2** as a function of the concentration of CCA. All reactions were run at 298 K in MeCN under air.

to acetophenone in 81 (±12)% yield. Styrene, the anticipated product from deformylation, is not observed. As with the CCA reaction, the reaction with 2-PPA is first-order with respect to the substrate (Figure S15). The reaction occurs at about the same rate, with a k_2 value of 1.7 (±0.3) × 10^{-2} M^{-1} s^{-1} (Figure S16).

Complex **2** also degrades in the presence of benzaldehydes (Figure S17). Regrettably, the organic product was not isolated and identified. Prior reports in this area have encountered similar difficulties,[28,29,36] suggesting that the initially generated organic products may react further. The reactivity was tested with four *para*-substituted benzaldehydes (Cl, H, F, Me) in MeCN at 298 K (Figure 3). The more electron-rich benzaldehydes, as assessed by their σ_p^+ values,[62] react with **2** more slowly, consistent with the Co(III)-peroxo complex serving as a nucleophile. A plot of log(k_{obs}) versus σ_p^+ yields a ρ value of 1.6.

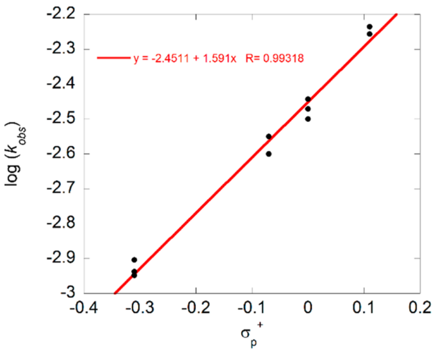

Figure 3. Hammett plot for the reactions between 2.0 mM **2** and 400 mM *para*-X-benzaldehydes (X = Cl, H, F, Me) under air in 298 K MeCN.[62] $\rho = 1.6$, $R^2 = 0.986$.

The identity of the initially generated cobalt-containing product regrettably remains unresolved. MS analysis of reactions between **2** and aldehydes show evidence of ligand decomposition (Figure S18).

Reactivity of the Species Generated from PhIO. Prior research found that certain Co(II) complexes could react with PhIO in the presence of a Lewis acid, such as Sc(III), to yield species capable of oxidizing DHA. Mixtures of complex **1** and PhIO are likewise capable of activating weak C−H bonds (Table 4); an additional Lewis acid beyond the Co(II), however, is not needed for this reactivity to proceed.

DHA is converted exclusively into anthracene; the time-dependent yields of anthracene suggest that the reaction completes in under 30 min. The oxygenated products anthrone and anthroquinone are not observed, and performing the reaction under N_2 has no significant impact on either the product distribution or the yield of anthracene. 1,4-Cyclohexadiene (CHD) is oxidized exclusively to benzene under both air and N_2. As with the DHA reactions, the CHD reactions are complete within 30 min and yield the same results under air and N_2. Xanthene is oxidized to xanthone. Under air but not N_2, the yields of xanthone are higher and continue to increase past 30 min. Neither fluorene, cyclohexane, cyclohexene, cumene, nor toluene react with **1** and PhIO to observable degrees. No oxidation of cyclohexane, cumene, or toluene is detected even when 500 mM of these substrates is added instead of our standard 50 mM.

The reactivity with DHA, CHD, and xanthene is notable in that it is catalytic, rather than stoichiometric, with respect to the cobalt. With excess PhIO, up to 12 equiv of anthracene per equiv of **1** can be produced, suggesting that the cobalt catalyst turns over 11 times. These substrates do not react with PhIO without a catalyst. The yield of anthracene maximizes within 30 min, which is again consistent with the catalyst degrading under the reaction conditions. The higher and increasing yields of xanthone under air suggests that this process partly proceeds through the propagation of organic radicals, rather than solely the regeneration of a metal-based oxidant, when O_2 is present.

Although Sc(III) or another Lewis acid was not needed to enable the catalysis, the necessity of such for prior cobalt-mediate C−H activation prompted us to investigate whether an additional Lewis acid could enhance the activity.[44,45,63] To our surprise, we found that the addition of Sc(OTf)$_3$ inhibited, rather than improved, the catalysis, and the yields of anthracene from DHA were noticeably lower when Sc(III) was present (Table 4). The product distribution remained unaltered, and no oxygenated organic products were found. The yield of anthracene at 120 min is essentially the same as that measured at 30 min, and it does not appear that the Sc(III) is either stabilizing the metal-based oxidant or otherwise prolonging the lifetime of the catalyst.

meta-Chloroperbenzoic acid (MCPBA) can substitute for PhIO as the terminal oxidant, but the yields of the oxidized hydrocarbons are generally lower (Table 5). MCPBA reacts directly with alkenes to yield epoxides, and 1,4-cyclohexene monoxide is observed in its reactions with **1** and CHD in addition to the anticipated benzene. We also investigated oxone, H_2O_2, *tert*-butylhydroperoxide, and air by itself as terminal oxidants but found no reactivity with organic substrates.

We explored using **1** as a catalyst for oxygen-atom-transfer reactions but found that mixtures of the Co(II) precursor and PhIO were unable to convert cyclohexene, cyclooctene, and α-methyl-styrene to the corresponding epoxides. Compound **1** was, however, able to catalyze the oxidation of Ph_3P to triphenylphosphine oxide (Ph_3PO) by PhIO. When 1.0 mM of **1** was used to catalyze the reaction between 25 mM PhIO and 50 mM Ph_3P in MeCN, Ph_3PO is formed quantitatively within 30 min (>99%, 25 TON). Unlike the hydrocarbon oxidation reactions, the Ph_3P reactions were followed by ^1H NMR. As has been found for other systems, the catalyst-free reaction between PhIO and Ph_3P did not yield any Ph_3PO.[64]

DOI: 10.1021/acs.inorgchem.6b02127
Inorg. Chem. XXXX, XXX, XXX−XXX

■ DISCUSSION

The bbpc ligand was previously used to stabilize a ferric hydroperoxide complex,[18,50,51] and we were curious as to whether the ligand could be used to stabilize other species relevant to metal−O_2 chemistry. Cobalt complexes with O_2 and related ligands, in particular, may have high mechanistic relevance in the cobalt-catalyzed O_2 production recently studied by Nocera and others.[12−14,65,66]

Structurally characterized cobalt(III) peroxo species are rare, but the few that have been observed have a diverse array of coordination spheres. Some of these adducts have been prepared from the reactions between cobalt(I) precursors and O_2;[56−58] others have been synthesized from reactions between cobalt(II) complexes, H_2O_2, and an added base.[29,56,59] The synthetic routes originating from cobalt(I) have thus far invariably contained softer base spectator ligands, resulting in As_4O_2, P_4O_2, and C_3NO_2 coordination spheres in the cobalt(III) products.[56−58] A cobalt(II) superoxo complex isolated from the reaction between a cobalt(I) starting material and O_2 also merits mention; this was distinguished from the aforementioned peroxo species on the bases of its noticeably shorter O−O bond and its ability to abstract hydrogen atoms from weak C−H bonds.[67] A recently characterized cobalt(III) superoxo complex was also found to abstract hydrogen atoms from TEMPO-H, resulting in a Co^{III}-OOH species.[49]

A cobalt(III) peroxo complex (**2**) was synthesized from the reaction between $[Co(bbpc)(MeCN)_2]^{2+}$ (**1**), H_2O_2, and Et_3N (Figure 1). The Co−N and Co−O bond lengths of **2** are consistent with a low-spin cobalt(III) metal center; the oxidation- and spin-state assignments are corroborated by the diamagnetic ^1H NMR spectrum (Figure S4) and the absence of an EPR signal. The O−O bond length is consistent with a peroxo ligand, as opposed to a superoxo or a bound O_2.[29,56−59,67] MS of samples of **2** in MeCN suggests that the solid-state structure is maintained in solution (Figure S11).

Much like some, but certainly not all, other isolated metal peroxo complexes, compound **2** stoichiometrically reacts with aldehydes (Table 3). When observed, these reactions typically yield mixtures of alkenes and ketones; the product distribution is highly dependent on the identities of both the coordination complex and the aldehyde.[28,29,31−34,36,68] In the cited cases, deformylation of the aldehyde to an alkene is sometimes found for CCA but has never been found for 2-PPA. Compound **2** can convert CCA to cyclohexene, but not to the same extent as a cobalt(III) peroxo complex with the 13-TMC ligand (Scheme 2).[29] The 13-TMC complex converts CCA exclusively to the alkene. Both compounds react with 2-PPA to yield acetophenone as the sole organic product. Despite the dissimilarity in their ligand structures, the two cobalt(III) peroxo compounds react with aldehydes at similar rates. This is notable because aldehyde deformylation was not observed for a cobalt(III) peroxo complex with the 12-TMC ligand in the absence of acid.[29,35] The k_2 values for the 13-TMC complex are 2.0×10^{-1} M^{-1} s^{-1} for CCA and 1.5×10^{-2} M^{-1} s^{-1} for 2-PPA.[29] Complex **2** reacts with CCA more slowly, with a k_2 value of 2.4×10^{-2} M^{-1} s^{-1}, but reacts at approximately the same rate with 2-PPA as a substrate, with a k_2 value of 1.7×10^{-2} M^{-1} s^{-1}. The Hammett plot derived from the reactions with derivatized benzaldehydes yields a ρ value of 1.6 (Figure 3). This is both similar to the 1.7 value found for the 13-TMC complex[29] and indicative of a nucleophilic reagent. The proposed mechanism for the reactivity with aldehydes is shown in Scheme 4; the same mechanism has been suggested for other transition-metal peroxo complexes.[28,34] Disappointingly, excesses of H_2O_2 and Et_3N do not result in catalytic aldehyde deformylation. The sole cobalt-containing catalyst for aldehyde deformylation instead appears to rely on a radical cobalt(II) superoxide species as the metal-based oxidant.[68]

Table 3. Oxidation of Substrates by 2[a]

substrate	product	yield (%)[b]
CCA	cyclohexene	26 (±6)
	cyclohexanol	63 (±10)
2-PPA (CHD)	acetophenone	81 (±12)
xanthene	no reaction	N.A.
DHA	no reaction	N.A.
cyclohexene	no reaction	N.A.

[a] Standard reaction conditions: All reactions were run at 298 K in 2.5 mL of MeCN under air for 60 min. The starting concentrations of **2** and substrate in all reactivity assays were 2.0 and 100 mM, respectively. Complex **2** was generated in situ from the reaction between 2.0 mM **1**, 10 mM H_2O_2, and 5.0 mM Et_3N.[29] The concentrations of each organic product were calibrated relative to that of an internal standard (dichlorobenzene) with a known concentration. [b] Complex **2** is the limiting reagent.

Scheme 4

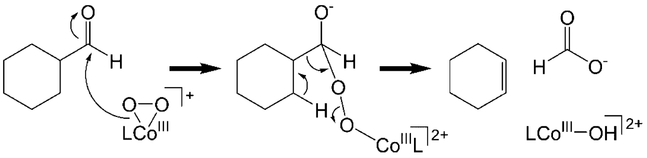

The reaction between **1** and PhIO generates another reactive cobalt complex with a distinct reactivity profile. A previous reaction between PhIO and another cobalt(II) complex produced a mixture of a Co^{II}-PhIO complex and a higher-valent species that was initially assigned as a cobalt(IV) oxo compound.[44] The addition of scandium triflate shifted the equilibrium position toward the oxidized cobalt. The reaction between PhIO, $Sc(OTf)_3$, and yet another cobalt(II) complex resulted in a Co^{III}-OH complex with structural, spectroscopic, and reactive similarities to the first higher-valent species, casting doubt on its assignment as a true cobalt(IV) compound.[45] A cobalt(IV) oxo complex with a tetraamido macrocyclic ligand (TAML) was reported from the reaction between PhIO, scandium(III), and a cobalt(III) precursor.[63] The TAML complex reacts with substrates with weak C−H bonds in a manner reminiscent of those of the first two cobalt oxidants.[44,45,63] Tilley and co-workers reported that a cobalt(II) complex with a tetraanionic ligand could activate the C−H bonds of MeCN using either O_2 or PhIO as the terminal oxidant; the difficulty of this transformation led them to propose that a transient cobalt(IV) species was responsible for oxidation of the solvent.[48]

The cobalt(II) complex **1** is capable of catalyzing the oxidation of weak C−H bonds by either PhIO or MCPBA, and the catalyst appears capable of turning over at least 10 times (Table 4). Although complex **1** is perhaps not quite ready for industrial use, the modest turnover is noteworthy because only stoichiometric reactivity had thus far been reported for the cobalt-mediated oxidation of DHA by PhIO.[44,45,48,63] C−H activation by MCPBA has not been reported with discrete

Table 4. Oxidation of Hydrocarbons by PhIO Catalyzed by 1[a]

substrate	atmosphere	time (min)	product	yield (%)[b]	TON[c]
DHA	air	30	anthracene	46 (±2), 10 (±2)[d]	12, 3.0[d]
		60		42 (±2), 8 (±2)[d]	10, 1.8[d]
		120		44 (±2), 10 (±2)[d]	11, 2.5[d]
	N_2	30	anthracene	42 (±2)	11
CHD	air	30	benzene	64 (±4)	16
	N_2	30	benzene	56 (±4)	14
Xanthene	air	30	xanthone	22 (±4)	6.0
		60		34 (±8)	8.5
		120		48 (±6)	12
	N_2	30	xanthone	12 (±4)	3.2
		60		12 (±2)	2.9
		120		14 (±2)	3.7

[a] Standard reaction conditions: All reactions were run at 298 K in 2.5 mL of MeCN. The starting concentrations of the cobalt(II) catalyst (**1**) and the substrate in all reactivity assays were 1.0 and 50 mM, respectively. A total of 25 equiv of PhIO, relative to the **1**, was added at the beginning of the reaction. For each time point, an aliquot of the reaction mixture was diluted with ether, filtered through silica gel, and analyzed via GC. The products were identified by comparing the retention times with those of authentic samples of anthracene, xanthone, and benzene. The concentrations of each organic product were calibrated relative to that of an internal standard (dichlorobenzene) with a known concentration. [b] PhIO is the limiting reagent. [c] Turnover number, defined as the number of moles of oxidized organic product generated per mole of **1**. [d] Reactions contain 1.0 mM Sc(OTf)$_3$ as an additive.

cobalt complexes, but it has been documented with iron compounds.[69,70] MCPBA poses a complication in that it can react directly with alkenes to yield epoxides, and indeed this activity is seen when CHD is used as the substrate. Despite this background reactivity, the cobalt catalyst does sufficiently shift the reactivity to yield benzene as the major product (Table 5).

Table 5. Oxidation of Hydrocarbons by MCPBA Catalyzed by 1[a]

substrate	atmosphere	time (min)	product	yield (%)[b]	TON[c]
DHA	air	30	anthracene	36 (±2)	8.8
	N_2	30	anthracene	28 (±4)	7.2
CHD	air	30	benzene	50 (±4)	13
			epoxide[d]	32 (±6)	
	N_2	30	benzene	50 (±6)	13
			epoxide[d]	26 (±4)	

[a] Standard reaction conditions: All reactions were run at 298 K in 2.5 mL of MeCN. The starting concentrations of the cobalt(II) catalyst (**1**) and the substrate in all reactivity assays were 1.0 and 50 mM, respectively. A total of 25 equiv of MCPBA, relative to the **1**, was added at the beginning of the reaction. For each time point, an aliquot of the reaction mixture was diluted with ether, filtered through silica gel, and analyzed via GC. The products were identified by comparing the retention times with those of authentic samples of anthracene, benzene, and 1,4-cyclohexadiene oxide. The 1,4-cyclohexadiene monoxide standard was synthesized from the uncatalyzed reaction between CHD and MCPBA. The concentrations of each organic product were calibrated relative to that of an internal standard (dichlorobenzene) with a known concentration. [b] MCPBA is the limiting reagent. [c] Turnover number, defined as the number of moles of oxidized organic product generated per mole of **1**. [d] 1,4-Cyclohexadiene monoxide.

The reactivity of our system is limited to substrates with weak C−H bonds.[44,45,48,63] The benzylic C−H bonds of DHA and xanthene have bond dissociation energies (BDEs) of approximately 78 and 75 kcal mol^{-1}, respectively.[71] The allylic C−H bonds of CHD have been estimated to have a BDE of 75 kcal mol^{-1}.[72] No oxidation is observed with even moderately stronger C−H bonds, such as the benzylic ones in fluorene and toluene. In the absence of an external substrate, the complex appears to oxidize itself, as evidenced by MS (Figure S12). The inability to generate the oxidant cleanly has thus far precluded both its characterization and a more thorough kinetic analysis of the C−H activation. Attempts to observe intermediates at low temperatures by either EPR or UV/vis have thus far been unsuccessful, even using the more soluble MCBPA as the terminal oxidant.

One key difference between most prior cobalt oxidants capable of C−H activation and our own is that a Lewis acid is not necessary for the reactivity. The current inability to isolate a higher-valent species from reaction mixtures of PhIO and **1** limits our ability to understand both why we observe catalysis and why an additive is not needed to achieve C−H activation. MS analysis of the reaction between **1** and PhIO found evidence for a Co^{III}-OH species, **3**, but this complex was not definitively detected by ^{1}H NMR. Given that Mn^{III}-OH and Fe^{III}-OH species have previously demonstrated similarly mild C−H activation chemistry,[20,73−75] we currently speculate that a Co^{III}-OH species could at least be partly responsible for C−H activation of the external substrates (Scheme 5). This species could abstract a hydrogen atom from a substrate with a suitably weak C−H bond to yield a Co^{II}-OH$_2$ species, which could subsequently be reoxidized to a higher-valent species by PhIO or MCPBA. Co^{III}-OH could conceivably form from a reaction between a hydrogen-atom donor (e.g., MeCN, bbpc ligand, external substrate) and a more reactive cobalt(IV) oxo species that could be generated from the direct reaction between PhIO and **1**. Unfortunately, we were unable to intercept a putative cobalt(IV) oxidant with a large excess of cyclohexane, which contains C−H bonds that would be too strong to be activated

Scheme 5

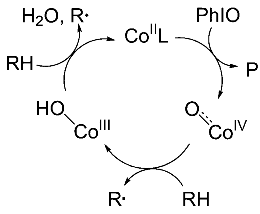

by other documented M^{III}-OH species.[20,73−75] We also attempted to generate a Co^{III}-OH species without the intermediacy of a cobalt(IV) oxidant by sequentially reacting **1** with hydroxide sources and ceric ammonium nitrate. Such reactions resulted in mixtures containing $[Co(bbpc)(NO_3)]^+$ and cobalt complexes with oxidized ligands. The inability to observe the Co^{III}-OH product anticipated from aldehyde deformylation (Figure S18) could also be explained by the Co^{III}-OH functional group oxidizing the benzylic C−H bonds of the bbpc ligand. Further investigation into these potential oxidants and their reactivity with hydrocarbon substrates is underway.

Valentine and co-workers had previously found that a variety of Lewis acid complexes were capable of catalyzing olefin epoxidation by PhIO.[76,77] This chemistry was observed even for redox-inactive metal ions such as zinc(II) and aluminum(III), leading them to propose that metal−PhIO complexes were the relevant oxidants.[76] Mixtures of **1** and PhIO, conversely, do not catalyze olefin epoxidation. This further supports the notion that Co^{II}-PhIO complexes are not particularly stable with the bbpc ligand. ^{1}H NMR analysis of the reactions between **1** and PhIO in the absence of substrate revealed PhI and unreacted PhIO (Figure S5), providing further evidence that the reaction can proceed past simple Co^{II}-PhIO complexes without Lewis acid additives.

CONCLUSIONS

A neutral nitrogen-donor ligand, bbpc, supports two distinct modes of reactivity with cobalt, with the choice of terminal oxidant determining the identity of the metal-based oxidant and the observed substrate reactivity. The addition of H_2O_2 and a base yields a cobalt(III) peroxo complex that is capable of reacting with aldehydes. PhIO and MCPBA, conversely, react with the cobalt(II) ion to form species capable of oxidizing weak C−H bonds. We currently believe that a Co^{III}-OH species is at least partly responsible for the oxidation of external substrates. The cobalt-driven C−H activation is noteworthy both for not requiring a Lewis acid to activate the terminal oxidant and for being catalytic, rather than stoichiometric.

ASSOCIATED CONTENT

Ⓢ Supporting Information

The Supporting Information is available free of charge on the ACS Publications website at DOI: 10.1021/acs.inorgchem.6b02127.

IR, MS, and NMR data, UV/vis spectra of the reaction between **2** and aldehyde substrates, and a plot of k_{obs} versus [2-PPA] for reactions between 2-PPA and **2** (PDF)

X-ray crystallographic data in CIF format (CIF)

AUTHOR INFORMATION

Corresponding Author

*E-mail: crgoldsmith@auburn.edu.

ORCID

Qiao Zhang: 0000-0002-6326-2556

Christian R. Goldsmith: 0000-0001-7293-1267

Notes

The authors declare no competing financial interest.

ACKNOWLEDGMENTS

The work described was financially supported by Auburn University and a grant from the American Chemical Society, Petroleum Research Fund (Grant 55301-ND3).

REFERENCES

(1) Costas, M.; Mehn, M. P.; Jensen, M. P.; Que, L., Jr. Dioxygen Activation at Mononuclear Nonheme Iron Active Sites: Enzymes, Models, and Intermediates. *Chem. Rev.* **2004**, *104*, 939−986.

(2) Que, L., Jr.; Ho, R. Y. N. Dioxygen Activation by Enzymes with Mononuclear Non-Heme Iron Active Sites. *Chem. Rev.* **1996**, *96*, 2607−2624.

(3) Mirica, L. M.; Ottenwaelder, X.; Stack, T. D. P. Structure and Spectroscopy of Copper-Dioxygen Complexes. *Chem. Rev.* **2004**, *104*, 1013−1045.

(4) Kryatov, S. V.; Rybak-Akimova, E. V.; Schindler, S. Kinetics and Mechanisms of Formation and Reactivity of Non-heme Iron Oxygen Intermediates. *Chem. Rev.* **2005**, *105*, 2175−2226.

(5) Collman, J. P.; Boulatov, R.; Sunderland, C. J.; Fu, L. Functional Analogues of Cytochrome c Oxidase, Myoglobin, and Hemoglobin. *Chem. Rev.* **2004**, *104*, 561−588.

(6) Kovaleva, E. G.; Neibergall, M. B.; Chakrabarty, S.; Lipscomb, J. D. Finding Intermediates in the O_2 Activation Pathways of Non-Heme Iron Oxygenases. *Acc. Chem. Res.* **2007**, *40*, 475−483.

(7) Hikichi, S.; Akita, M.; Moro-oka, Y. New Aspects of the Cobalt-Dioxygen Complex Chemistry Opened by Hydrotris(pyrazoly)borate Ligands (Tp^R): Unique Properties of Tp^RCo-Dioxygen Complexes. *Coord. Chem. Rev.* **2000**, *198*, 61−87.

(8) Park, Y. J.; Ziller, J. W.; Borovik, A. S. The Effects of Redox-Inactive Metal Ions on the Activation of Dioxygen: Isolation and Characterization of a Heterobimetallic Complex Containing a $Mn^{III}(\mu$-OH)-Ca^{II} Core. *J. Am. Chem. Soc.* **2011**, *133*, 9258−9261.

(9) Park, Y. J.; Cook, S. A.; Sickerman, N. S.; Sano, Y.; Ziller, J. W.; Borovik, A. S. Heterobimetallic Complexes with M^{III}-(μ-OH)-M^{II} Cores (M^{III} = Fe, Mn, Ga; M^{II} = Ca, Sr, and Ba): Structural, Kinetic, and Redox Properties. *Chem. Sci.* **2013**, *4*, 717−726.

(10) Suzuki, M. Ligand Effects on Dioxygen Activation by Copper and Nickel Complexes: Reactivity and Intermediates. *Acc. Chem. Res.* **2007**, *40*, 609−617.

(11) Wang, D.; Groves, J. T. Efficient Water Oxidation Catalyzed by Homogeneous Cationic Cobalt Porphyrins with Critical Roles for the Buffer Base. *Proc. Natl. Acad. Sci. U. S. A.* **2013**, *110*, 15579−15584.

(12) Barats-Damatov, D.; Shimon, L. J. W.; Weiner, L.; Schreiber, R. E.; Jiménez-Lozano, P.; Poblet, J. M.; de Graaf, C.; Neumann, R. Dicobalt-μ-oxo Polyoxometalate Compound, $[(\alpha_2\text{-}P_2W_{17}O_{61}Co)_2O]^{14-}$: A Potent Species for Water Oxidation, C-H Bond Activation, and Oxygen Transfer. *Inorg. Chem.* **2014**, *53*, 1779−1787.

(13) Surendranath, Y.; Kanan, M. W.; Nocera, D. G. Mechanistic Studies of the Oxygen Evolution Reaction by a Cobalt-Phosphate Catalyst at Neutral pH. *J. Am. Chem. Soc.* **2010**, *132*, 16501−16509.

(14) Symes, M. D.; Surendranath, Y.; Lutterman, D. A.; Nocera, D. G. Bidirectional and Unidirectional PCET in a Molecular Model of a Cobalt-Based Oxygen-Evolving Catalyst. *J. Am. Chem. Soc.* **2011**, *133*, 5174−5177.

(15) Brunschwig, B. S.; Chou, M. H.; Creutz, C.; Ghosh, P.; Sutin, N. Mechanisms of Water Oxidation to Oxygen: Cobalt(IV) as an Intermediate in the Aquocobalt(II)-Catalyzed Reaction. *J. Am. Chem. Soc.* **1983**, *105*, 4832−4833.

(16) Betley, T. A.; Wu, Q.; Van Voorhis, T.; Nocera, D. G. Electronic Design Criteria for O-O Bond Formation via Metal-Oxo Complexes. *Inorg. Chem.* **2008**, *47*, 1849−1861.

(17) Sharma, S. K.; May, P. S.; Jones, M. B.; Lense, S.; Hardcastle, K. I.; MacBeth, C. E. Catalytic Dioxygen Activation by Co(II) Complexes Employing a Coordinatively Versatile Ligand Scaffold. *Chem. Commun.* **2011**, *47*, 1827−1829.

(18) He, Y.; Goldsmith, C. R. Observation of a Ferric Hydroperoxide Complex during the Non-heme Iron Catalysed Oxidation of Alkenes and Alkanes by O_2. *Chem. Commun.* **2012**, *48*, 10532−10534.

(19) Lee, Y.-M.; Hong, S.; Morimoto, Y.; Shin, W.; Fukuzumi, S.; Nam, W. Dioxygen Activation by a Non-Heme Iron(II) Complex: Formation of an Iron(IV)-Oxo Complex via C-H Activation by a Putative Iron(III)-Superoxo Species. *J. Am. Chem. Soc.* **2010**, *132*, 10668−10670.

(20) Gupta, R.; Borovik, A. S. Monomeric $Mn^{III/II}$ and $Fe^{III/II}$ Complexes with Terminal Hydroxo and Oxo Ligands: Probing Reactivity via O-H Bond Dissociation Energies. *J. Am. Chem. Soc.* **2003**, *125*, 13234−13242.

(21) Jaafar, H.; Vileno, B.; Thibon, A.; Mandon, D. Tuning the Conversion of Cyclohexane into Cyclohexanol/one by Molecular Dioxygen, Protons and Reducing Agents at a Single Non-Porphyrinic Iron Centre and Chemical Versatility of the Tris(2-pyridylmethyl)-amine $TPAFe^{II}Cl_2$ Complex in Mild Oxidation Chemistry. *Dalton Trans.* **2011**, *40*, 92−106.

(22) Mukherjee, A.; Martinho, M.; Bominaar, E. L.; Münck, E.; Que, L., Jr. Shape-Selective Interception by Hydrocarbons of the O_2-Derived Oxidant of a Biomimetic Nonheme Iron Complex. *Angew. Chem., Int. Ed.* **2009**, *48*, 1780−1783.

(23) Mukherjee, J.; Lucas, R. L.; Zart, M. K.; Powell, D. R.; Day, V. W.; Borovik, A. S. Synthesis, Structure, and Physical Properties for a Series of Monomeric Iron(III) Hydroxo Complexes with Varying Hydrogen-Bond Networks. *Inorg. Chem.* **2008**, *47*, 5780−5786.

(24) Rohde, J.-U.; In, J.-H.; Lim, M. H.; Brennessel, W. W.; Bukowski, M. R.; Stubna, A.; Münck, E.; Nam, W.; Que, L., Jr. Crystallographic and Spectroscopic Characterization of a Nonheme Fe(IV)═O Complex. *Science* **2003**, *299*, 1037−1039.

(25) Fukuzumi, S.; Morimoto, Y.; Kotani, H.; Naumov, P.; Lee, Y.-M.; Nam, W. Crystal Structure of a Metal Ion-Bound Oxoiron(IV) Complex and Implications for Biological Electron Transfer. *Nat. Chem.* **2010**, *2*, 756−759.

(26) Chen, J.; Lee, Y.-M.; Davis, K. M.; Wu, X.; Seo, M. S.; Cho, K.-B.; Yoon, H.; Park, Y. J.; Fukuzumi, S.; Pushkar, Y. N.; Nam, W. A Mononuclear Non-Heme Manganese(IV)-Oxo Complex Binding Redox-Inactive Metal Ions. *J. Am. Chem. Soc.* **2013**, *135*, 6388−6391.

(27) Kim, D.; Cho, J.; Lee, Y.-M.; Sarangi, R.; Nam, W. Synthesis, Characterization, and Reactivity of Cobalt(III)-Oxygen Complexes Bearing a Macrocyclic N-Tetramethylated Cyclam Ligand. *Chem. - Eur. J.* **2013**, *19*, 14112−14118.

(28) Cho, J.; Sarangi, R.; Nam, W. Mononuclear Metal-O_2 Complexes Bearing Macrocyclic *N*-Tetramethylated Cyclam Ligands. *Acc. Chem. Res.* **2012**, *45*, 1321−1330.

(29) Cho, J.; Sarangi, R.; Kang, H. Y.; Lee, J. Y.; Kubo, M.; Ogura, T.; Solomon, E. I.; Nam, W. Synthesis, Structural, and Spectroscopic Characterization and Reactivities of Mononuclear Cobalt(III)-Peroxo Complexes. *J. Am. Chem. Soc.* **2010**, *132*, 16977−16986.

(30) Sarangi, R.; Cho, J.; Nam, W.; Solomon, E. I. XAS and DFT Investigation of Mononuclear Cobalt(III) Peroxo Complexes: Electronic Control of the Geometric Structure in CoO_2 versus NiO_2 Systems. *Inorg. Chem.* **2011**, *50*, 614−620.

(31) Cho, J.; Jeon, S.; Wilson, S. A.; Liu, L. V.; Kang, E. A.; Braymer, J. J.; Lim, M. H.; Hedman, B.; Hodgson, K. O.; Valentine, J. S.; Solomon, E. I.; Nam, W. Structure and Reactivity of a Mononuclear Non-Haem Iron(III)-Peroxo Complex. *Nature* **2011**, *478*, 502−505.

(32) Annaraj, J.; Suh, Y.; Seo, M. S.; Kim, S. O.; Nam, W. Mononuclear Nonheme Ferric-Peroxo Complex in Aldehyde Deformylation. *Chem. Commun.* **2005**, 4529−4531.

(33) Annaraj, J.; Cho, J.; Lee, Y.-M.; Kim, S. Y.; Latifi, R.; de Visser, S. P.; Nam, W. Structural Characterization and Remarkable Axial Ligand Effect on the Nucleophilic Reactivity of a Nonheme Manganese(III)-Peroxo Complex. *Angew. Chem., Int. Ed.* **2009**, *48*, 4150−4153.

(34) Seo, M. S.; Kim, J. Y.; Annaraj, J.; Kim, Y.; Lee, Y.-M.; Kim, S.-J.; Kim, J.; Nam, W. $[Mn(tmc)(O_2)]^+$: A Side-On Peroxido Manganese-(III) Complex Bearing a Non-Heme Ligand. *Angew. Chem., Int. Ed.* **2007**, *46*, 377−380.

(35) Tcho, W.-Y.; Wang, B.; Lee, Y.-M.; Cho, K.-B.; Shearer, J.; Nam, W. A Mononuclear Nonheme Cobalt(III)-Hydroperoxide Complex with an Amphoteric Reactivity in Electrophilic and Nucleophilic Oxidative Reactions. *Dalton Trans.* **2016**, *45*, 14511−14515.

(36) Geiger, R. A.; Chattopadhyay, S.; Day, V. W.; Jackson, T. A. Nucleophilic Reactivity of a Series of Peroxomanganese(III) Complexes Supported by Tetradentate Aminopyridyl Ligands. *Dalton Trans.* **2011**, *40*, 1707−1715.

(37) Ray, K.; England, J.; Fiedler, A. T.; Martinho, M.; Münck, E.; Que, L., Jr. An Inverted and More Oxidizing Isomer of $[Fe^{IV}(O)(tmc)(NCCH_3)]^{2+}$. *Angew. Chem., Int. Ed.* **2008**, *47*, 8068−8071.

(38) Kim, S. O.; Sastri, C. V.; Seo, M. S.; Kim, J.; Nam, W. Dioxygen Activation and Catalytic Aerobic Oxidation by a Mononuclear Nonheme Iron(II) Complex. *J. Am. Chem. Soc.* **2005**, *127*, 4178−4179.

(39) Lim, M. H.; Rohde, J.-U.; Stubna, A.; Bukowski, M. R.; Costas, M.; Ho, R. Y. N.; Münck, E.; Nam, W.; Que, L., Jr. An Fe^{IV}═O Complex of a Tetradentate Tripodal Nonheme Ligand. *Proc. Natl. Acad. Sci. U. S. A.* **2003**, *100*, 3665−3670.

(40) Kaizer, J.; Klinker, E. J.; Oh, N. Y.; Rohde, J.-U.; Song, W. J.; Stubna, A.; Kim, J.; Münck, E.; Nam, W.; Que, L., Jr. Nonheme $Fe^{IV}O$ Complexes That Can Oxidize the C-H Bonds of Cyclohexane at Room Temperature. *J. Am. Chem. Soc.* **2004**, *126*, 472−473.

(41) Parsell, T. H.; Behan, R. K.; Green, M. T.; Hendrich, M. P.; Borovik, A. S. Preparation and Properties of a Monomeric Mn^{IV}-Oxo Complex. *J. Am. Chem. Soc.* **2006**, *128*, 8728−8729.

(42) Lacy, D. C.; Gupta, R.; Stone, K. L.; Greaves, J.; Ziller, J. W.; Hendrich, M. P.; Borovik, A. S. Formation, Structure, and EPR Detection of a High Spin Fe^{IV}-Oxo Species Derived from Either an Fe^{III}-Oxo or Fe^{III}-OH Complex. *J. Am. Chem. Soc.* **2010**, *132*, 12188−12190.

(43) Ghosh, M.; Singh, K. K.; Panda, C.; Weitz, A.; Hendrich, M. P.; Collins, T. J.; Dhar, B. B.; Sen Gupta, S. Formation of a Room Temperature Stable $Fe^V(O)$ Complex: Reactivity Toward Unactivated C-H Bonds. *J. Am. Chem. Soc.* **2014**, *136*, 9524−9527.

(44) Pfaff, F. F.; Kundu, S.; Risch, M.; Pandian, S.; Heims, F.; Pryjomska-Ray, I.; Haack, P.; Metzinger, R.; Bill, E.; Dau, H.; Comba, P.; Ray, K. An Oxocobalt(IV) Complex Stabilized by Lewis Acid Interactions with Scandium(III) Ions. *Angew. Chem., Int. Ed.* **2011**, *50*, 1711−1715.

(45) Lacy, D. C.; Park, Y. J.; Ziller, J. W.; Yano, J.; Borovik, A. S. Assembly and Properties of Heterobimetallic $Co^{II/III}/Ca^{II}$ Complexes with Aquo and Hydroxo Ligands. *J. Am. Chem. Soc.* **2012**, *134*, 17526−17535.

(46) O'Halloran, K. P.; Zhao, C.; Ando, N. S.; Schultz, A. J.; Koetzle, T. F.; Piccoli, P. M. B.; Hedman, B.; Hodgson, K. O.; Bobyr, E.; Kirk, M. L.; Knottenbelt, S.; Depperman, E. C.; Stein, B.; Anderson, T. M.; Cao, R.; Geletii, Y. V.; Hardcastle, K. I.; Musaev, D. G.; Neiwert, W. A.; Fang, X.; Morokuma, K.; Wu, S.; Kögerler, P.; Hill, C. L. Revisiting the Polyoxometalate-Based Late-Transition-Metal-Oxo Complexes: The "Oxo Wall" Stands. *Inorg. Chem.* **2012**, *51*, 7025−7031.

(47) Winkler, J. R.; Gray, H. B. Electronic Structures of Oxo-Metal Ions. *Struct. Bonding (Berlin, Ger.)* **2012**, *142*, 17−28.

(48) Nguyen, A. I.; Hadt, R. G.; Solomon, E. I.; Tilley, T. D. Efficient C-H Bond Activations via O_2 Cleavage by a Dianionic Cobalt(II) Complex. *Chem. Sci.* **2014**, *5*, 2874−2878.

(49) Wang, C.-C.; Chang, H.-C.; Lai, Y.-C.; Fang, H.; Li, C.-C.; Hsu, H.-K.; Li, Z.-Y.; Lin, T.-S.; Kuo, T.-S.; Neese, F.; Ye, S.; Chiang, Y.-W.; Tsai, M.-L.; Liaw, W.-F.; Lee, W.-Z. A Structurally Characterized Nonheme Cobalt−Hydroperoxo Complex Derived from Its Superoxo Intermediate via Hydrogen Atom Abstraction. *J. Am. Chem. Soc.* **2016**, *138*, 14186−14189.

(50) He, Y.; Gorden, J. D.; Goldsmith, C. R. Steric Modifications Tune the Regioselectivity of the Alkane Oxidation Catalyzed by Non-Heme Iron Complexes. *Inorg. Chem.* **2011**, *50*, 12651−12660; Addition/Correction. *Inorg. Chem.* **2012**, *51*, 7431.

(51) Zhang, Q.; Goldsmith, C. R. Kinetic Analysis of the Formation and Decay of a Non-Heme Ferric Hydroperoxide Species Susceptible to O-O Bond Homolysis. *Inorg. Chem.* **2014**, *53*, 5206−5211.

DOI: 10.1021/acs.inorgchem.6b02127

(52) Bain, G. A.; Berry, J. F. Diamagnetic Corrections and Pascal's Constants. *J. Chem. Educ.* **2008**, *85*, 532−536.

(53) Kennedy, F. S.; Hill, H. A. O.; Kaden, T. A.; Vallee, B. L. Electron Paramagnetic Resonance Spectra of Some Active Cobalt(II) Substituted Metalloenzymes and Other Cobalt(II) Complexes. *Biochem. Biophys. Res. Commun.* **1972**, *48*, 1533−1539.

(54) Drago, R. S. *Physical Methods for Chemists*, 2nd ed.; Surfside Scientific Publishers: Gainesville, FL, 1992.

(55) de Souza, I. C. A.; Faro, L. V.; Pinheiro, C. B.; Gonzaga, D. T. G.; da Silva, F. d. C.; Ferreira, V. F.; Miranda, F. d. S.; Scarpellini, M.; Lanznaster, M. Investigation of Cobalt(III)-Triazole Systems as Prototypes for Hypoxia-Activated Drug Delivery. *Dalton Trans.* **2016**, *45*, 13671−13674.

(56) Crump, D. B.; Stepaniak, R. F.; Payne, N. C. Charge Distribution in Dioxygen Complexes of Cobalt(III). The Crystal Structure and Absolute Configuration of $(+)_{546}$-Δ-*cis*-*β*-[{2,13-Dimethyl-6,9-diphenyl-2,6,9,13-tetraarsatetradecane}(dioxygen)cobalt-(III)] Perchlorate. *Can. J. Chem.* **1977**, *55*, 438−446.

(57) Hu, X.; Castro-Rodriguez, I.; Meyer, K. Dioxygen Activation by a Low-Valent Cobalt Complex Employing a Flexible Tripodal N-Heterocyclic Carbene Ligand. *J. Am. Chem. Soc.* **2004**, *126*, 13464−13473.

(58) Terry, N. W., III; Amma, E. L.; Vaska, L. Molecular Oxygen Binding in a Monomeric Cobalt Complex. The Crystal and Molecular Structure of Dioxygen-Bis[*cis*-1,2-bis(diphenylphosphino)ethylene]-cobalt Tetrafluoroborate. *J. Am. Chem. Soc.* **1972**, *94*, 653−655.

(59) Rahman, A. F. M. M.; Jackson, W. G.; Willis, A. C. The First Sideways-Bonded Peroxo Complex for a Tetraaminecobalt(III) Species. *Inorg. Chem.* **2004**, *43*, 7558−7560.

(60) Shannon, R. D. Revised Effective Ionic Radii and Systematic Studies of Interatomic Distances in Halides and Chalcogenides. *Acta Crystallogr., Sect. A: Cryst. Phys., Diffr., Theor. Gen. Crystallogr.* **1976**, *32*, 751−767.

(61) Zielinska, A.; Skulski, L. A Solvent-Free Synthesis of (Dichloroiodo)arenes from Iodoarenes. *Tetrahedron Lett.* **2004**, *45*, 1087−1089.

(62) Hansch, C.; Leo, A.; Taft, R. W. A Survey of Hammett Substituent Constants and Resonance and Field Parameters. *Chem. Rev.* **1991**, *91*, 165−195.

(63) Hong, S.; Pfaff, F. F.; Kwon, E.; Wang, Y.; Seo, M.-S.; Bill, E.; Ray, K.; Nam, W. Spectroscopic Capture and Reactivity of a Low-Spin Cobalt(IV)-Oxo Complex Stabilized by Binding Redox-Inactive Metal Ions. *Angew. Chem., Int. Ed.* **2014**, *53*, 10403−10407.

(64) Guillet, G. L.; Gordon, J. B.; Di Francesco, G. N.; Calkins, M. W.; Čižmár, E.; Abboud, K. A.; Meisel, M. W.; García-Serres, R.; Murray, L. J. A Family of Tri- and Dimetallic Pyridine Dicarboxamide Cryptates: Unusual *O*,*N*,*O*-Coordination and Facile Access to Secondary Coordination Sphere Hydrogen Bonding Interactions. *Inorg. Chem.* **2015**, *54*, 2691−2704.

(65) Reece, S. Y.; Hamel, J. A.; Sung, K.; Jarvi, T. D.; Esswein, A. J.; Pijpers, J. J. H.; Nocera, D. G. Wireless Solar Water Splitting Using Silicon-Based Semiconductors and Earth-Abundant Catalysts. *Science* **2011**, *334*, 645−648.

(66) Kanan, M. W.; Nocera, D. G. In Situ Formation of an Oxygen-Evolving Catalyst in Neutral Water Containing Phosphate and Co^{2+}. *Science* **2008**, *321*, 1072−1075.

(67) Egan, J. W., Jr.; Haggerty, B. S.; Rheingold, A. L.; Sendlinger, S. C.; Theopold, K. H. Crystal Structure of a Side-on Superoxo Complex of Cobalt and Hydrogen Abstraction by a Reactive Terminal Oxo Ligand. *J. Am. Chem. Soc.* **1990**, *112*, 2445−2446.

(68) Corcos, A. R.; Villanueva, O.; Walroth, R. C.; Sharma, S. K.; Bacsa, J.; Lancaster, K. M.; MacBeth, C. E.; Berry, J. F. Oxygen Activation by Co(II) and a Redox Non-Innocent Ligand: Spectroscopic Characterization of a Radical−Co(II)−Superoxide Complex with Divergent Catalytic Reactivity. *J. Am. Chem. Soc.* **2016**, *138*, 1796−1799.

(69) McDonald, A. R.; Bukowski, M. R.; Farquhar, E. R.; Jackson, T. A.; Koehntop, K. D.; Seo, M. S.; De Hont, R. F.; Stubna, A.; Halfen, J. A.; Münck, E.; Nam, W.; Que, L., Jr. Sulfur versus Iron Oxidation in an Iron−Thiolate Model Complex. *J. Am. Chem. Soc.* **2010**, *132*, 17118−17129.

(70) Cho, K.; Leeladee, P.; McGown, A. J.; DeBeer, S.; Goldberg, D. P. A High-Valent Iron−Oxo Corrolazine Activates C−H Bonds via Hydrogen-Atom Transfer. *J. Am. Chem. Soc.* **2012**, *134*, 7392−7399.

(71) Bordwell, F. G.; Cheng, J.-P.; Ji, G.-Z.; Satish, A. V.; Zhang, X. Bond Dissociation Energies in DMSO Related to the Gas Phase. *J. Am. Chem. Soc.* **1991**, *113*, 9790−9795.

(72) Burkey, T. J.; Majewski, M.; Griller, D. Heats of Formation of Radicals and Molecules by a Photoacoustic Technique. *J. Am. Chem. Soc.* **1986**, *108*, 2218−2221.

(73) Goldsmith, C. R.; Cole, A. P.; Stack, T. D. P. C-H Activation by a Mononuclear Manganese(III) Hydroxide Complex: Synthesis and Characterization of a Manganese-Lipoxygenase Mimic? *J. Am. Chem. Soc.* **2005**, *127*, 9904−9912.

(74) Goldsmith, C. R.; Stack, T. D. P. Hydrogen Atom Abstraction by a Mononuclear Ferric Hydroxide Complex: Insights into the Reactivity of Lipoxygenase. *Inorg. Chem.* **2006**, *45*, 6048−6055.

(75) Gupta, R.; MacBeth, C. E.; Young, V. G., Jr.; Borovik, A. S. Isolation of Monomeric $Mn^{III/II}$-OH and Mn^{III}-O Complexes from Water: Evaluation of O-H Bond Dissociation Energies. *J. Am. Chem. Soc.* **2002**, *124*, 1136−1137.

(76) Yang, Y.; Diederich, F.; Valentine, J. S. Lewis Acid Catalysts for Olefin Epoxidation by Iodosylbenzene. *J. Am. Chem. Soc.* **1991**, *113*, 7195−7205.

(77) Nam, W.; Valentine, J. S. Zinc(II) Complexes and Aluminum-(III) Porphyrin Complexes Catalyze the Epoxidation of Olefins by Iodosylbenzene. *J. Am. Chem. Soc.* **1990**, *112*, 4977−4979.